

Contract-Governed Training for Earth Observation: Observed Service Agreement Graphs and Coverage–Accuracy Trade-offs

Wenzhang Du

Department of Computer Engineering,
Mahanakorn University of Technology International College (MUTIC),
Bangkok, Thailand
Email: dqswordman@gmail.com

Abstract

Earth observation (EO) models are frequently trained under implicit sampling policies that optimize global accuracy but provide no explicit guarantees on who (which regions, classes, or mission-critical strata) is being served throughout training. This paper introduces a contract-governed training paradigm for EO in which training samples are grouped into service contracts—semantically meaningful units such as (dataset, region, rare-crop indicator)—and each contract is assigned a target service share. We instantiate this paradigm as an Observed Service Agreement Graph (OSAG), a lightweight governance layer that (i) monitors contract-level exposure (coverage) during optimization, (ii) drives empirical coverage toward target shares via contract-normalized sampling weights, and (iii) exposes explicit accuracy–governance trade-offs through two knobs: a sampling mixture coefficient α and a contract-regularization weight λ_C . We provide a compact theory in a toy setting: OSAG sampling concentrates empirical coverage to targets; coverage deviations upper-bound service-risk deviations; and contract design (coarse vs. fine) modulates governance cost. Experiments on AVIRIS hyperspectral scenes (Indian Pines + Salinas) and multispectral Sentinel-2 EuroSAT demonstrate that OSAG can substantially reduce priority coverage error while maintaining global accuracy and improving high-priority accuracy. A EuroSAT coarse-vs.-fine contract ablation further evidences how semantically refined contracts can reduce the accuracy cost per unit of governance improvement.

Keywords Earth observation, dataset governance, sampling, hyperspectral imaging, class imbalance, fairness, contract-level coverage.

1 Introduction

Modern EO pipelines increasingly operate under service-driven constraints: rare crop types must be reliably monitored, urban hot-spots require prioritized coverage, and multi-region deployments demand predictable attention allocation. However, conventional training procedures implicitly “serve” data according to observed frequencies (or class reweighting heuristics), offering no explicit mechanism to ensure that mission-critical strata are consistently and proportionally addressed.

This motivates a governance-oriented view of training: in addition to overall accuracy, we quantify and control contract-level service coverage—how often each semantically defined contract is exposed to the learner. While adjacent areas such as class-imbalance handling [9], curriculum learning [10], prioritized sampling [11], and distributionally robust training [12] offer partial solutions, they

typically optimize proxy objectives (e.g., long-tail accuracy) rather than directly enforcing service agreements over semantic units relevant to EO operations.

We propose Observed Service Agreement Graphs (OSAG): contracts define nodes (optionally with adjacency edges), and training induces observed node weights via exposure counts; OSAG partitions data into contracts, monitors coverage, and enables explicit trade-offs between predictive utility and governance objectives. Our results show that:

- OSAG can reduce priority coverage error by large margins on both hyperspectral and multi-spectral datasets while preserving global accuracy.
- OSAG improves high-priority accuracy (accuracy on priority contracts) with minimal global accuracy loss.
- Contract design matters: a EuroSAT coarse-vs.-fine ablation demonstrates that semantically refined contracts can reduce the governance cost, consistent with our theory.

Contributions:

- Contract-governed EO training: a practical framework to define, monitor, and control contract-level service.
- OSAG mechanism: contract-normalized sampling with explicit trade-off knobs α and λ_C .
- Toy theory: coverage concentration, risk bound, and a contract-design effect on governance cost.
- Evidence on HSI/MSI: Indian+Salinas and EuroSAT, plus coarse/fine ablation.

2 Problem Setup: Contracts, Coverage, and Service Risk

2.1 Contracts and target service shares

Let training data be partitioned into m contracts $C = \{1, \dots, m\}$. Each contract c corresponds to a semantically meaningful unit. In our experiments:

- Indian+Salinas (HSI): contract \approx (dataset-id, spatial grid cell, rare-class flag).
- EuroSAT (MSI): contract \approx semantic groupings of classes, with a coarse vs. fine refinement for ablation.

Each contract c has n_c samples and a target service share $w_c > 0$ such that $\sum_c w_c = 1$. Target shares implement governance policy (e.g., higher share for rare crops or critical regions), paralleling classical resource allocation objectives where fairness or priority can be encoded via target proportions [18].

2.2 Empirical coverage and priority coverage error

Let C_t denote the contract served at training step $t = 1, \dots, T$. The empirical coverage is

$$\hat{q}_T(c) = \frac{1}{T} \sum_{t=1}^T \mathbb{1}\{C_t = c\}. \tag{1}$$

Coverage error uses the L_1 deviation from target:

$$E_{\text{cov}}(T) = \|\hat{q}_T - w\|_1 = \sum_c |\hat{q}_T(c) - w_c|. \tag{2}$$

In EO governance, the key is not only uniformity but adherence to priority targets, so we report priority coverage error relative to a priority-weighted target distribution.

2.3 Contract-level service risk

Let f_θ be the model and $\ell(\cdot, \cdot)$ a standard loss (cross-entropy). Define average loss on contract c :

$$\ell_\theta(c) = \frac{1}{n_c} \sum_{(x,y) \in D_c} \ell(f_\theta(x), y). \quad (3)$$

For a contract distribution q , define service risk

$$R_\theta(q) = \sum_c q(c) \ell_\theta(c). \quad (4)$$

This makes governance explicit: changing the coverage distribution changes the risk being optimized and the populations being effectively served.

3 OSAG: Governance via Contract-Normalized Sampling

OSAG implements a target contract distribution at the sampling layer. At each step:

- sample a contract c with probability w_c ;
- sample uniformly within D_c .

Equivalently, each sample i in contract c receives weight proportional to w_c/n_c . This yields an implementable weighted sampler conceptually related to prioritized sampling [11] but with policy-defined contract targets rather than TD-error heuristics.

3.1 Trade-off knob 1: sampling mixture α

To avoid overly aggressive governance, we mix baseline sampling and OSAG sampling:

- with probability α : sample according to OSAG weights;
- with probability $1 - \alpha$: sample from a baseline distribution (e.g., uniform over samples or a baseline policy).

This allows a continuous path between purely utility-driven training and purely contract-governed training.

3.2 Trade-off knob 2: contract regularization λ_C

We also support a simple contract-aware loss modulation:

$$\ell_{\text{total}} = \ell_{\text{CE}} + \lambda_C \cdot \Omega(\text{priority}, \ell_{\text{CE}}), \quad (5)$$

where Ω is a lightweight regularizer that increases pressure on priority contracts, echoing group-robust or constrained optimization ideas [12–14].

4 Toy Theory (Compact): Why Coverage Control Matters

Proposition 1 (Coverage concentration under OSAG sampling). Assume $\{C_t\}$ are i.i.d. with $\Pr(C_t = c) = w_c$. Then $\hat{q}_T(c) \rightarrow w_c$ almost surely for each c , and for any $\epsilon > 0$,

$$\Pr(|\hat{q}_T(c) - w_c| \geq \epsilon) \leq 2 \exp(-2T\epsilon^2). \quad (6)$$

By union bound, $\Pr(E_{\text{cov}}(T) \geq m\epsilon) \leq 2m \exp(-2T\epsilon^2)$. Implication: OSAG is a principled mechanism to drive coverage error down as training progresses, which is exactly what PrioCovErr measures.

Proposition 2 (Service-risk deviation is bounded by coverage error). Assume a bounded loss (e.g., 0–1 error or clipped cross-entropy) so that $0 \leq \ell_\theta(c) \leq B$ for all c ; then for any two contract distributions q, \tilde{q} ,

$$|R_\theta(q) - R_\theta(\tilde{q})| \leq B \|q - \tilde{q}\|_1. \quad (7)$$

Implication: once a final contract-loss vector is realized, coverage error directly upper-bounds how far actual service risk departs from the intended policy.

Proposition 3 (Contract design modulates governance cost). Introduce a contract adjacency graph $G = (C, E)$. If contract losses are β -Lipschitz on G in shortest-path distance, then letting $c^* = \arg \min_c \ell_\theta(c)$ yields

$$\max_c \ell_\theta(c) \leq \ell_\theta(c^*) + \beta \text{diam}(G), \quad (8)$$

and thus

$$|R_\theta(q) - R_\theta(\tilde{q})| \leq (\ell_\theta(c^*) + \beta \text{diam}(G)) \|q - \tilde{q}\|_1. \quad (9)$$

Implication: governance cost depends not only on how many contracts exist but on how semantically coherent they are (captured in β) and their induced structure. A refined contract design can reduce β by reducing within-contract heterogeneity, potentially lowering the accuracy penalty per unit of governance improvement—exactly what our coarse-vs.-fine EuroSAT study probes.

5 Experimental Protocol

5.1 Datasets

Indian Pines + Salinas (AVIRIS hyperspectral) are widely used HSI benchmarks [3–5]. Bands are aligned across scenes by selecting the shared subset (standard practice). EuroSAT-MSI (Sentinel-2 multispectral) is a common EO benchmark [1, 2]. We use the 13-band MSI setting with a consistent vector representation.

5.2 Representation and model (architecture-orthogonal evaluation)

To isolate the governance effect from backbone choice (CNN/ViT/etc. [8]) rather than stronger spectral–spatial CNNs [6, 7], we use a simple consistent classifier family:

- HSI: per-labeled pixel spectral vector (aligned to common bands across scenes).
- EuroSAT MSI: per-patch band-mean vector (13-D).

A lightweight MLP is trained with AdamW [15] (Adam [16] as the base formulation). This design ensures that improvements in coverage and high-priority performance can be attributed to the governance layer rather than model capacity.

5.3 Contract definitions and priority targets

HSI (Indian+Salinas): contracts capture dataset identity, coarse geography (grid cell), and rare-class indicator; rare or critical subgroups receive higher target shares. EuroSAT: contracts capture semantic class groupings; for Proposition 3, we implement a coarse contract set and a fine refinement (more contracts), then compare governance arrows baseline→OSAG.

Table 1: Operating points (mean \pm std, 3 seeds). Rare: bottom 20% frequency; priority $\in \{1, 3\}$ (rare=3); targets $w_c \propto \text{priority}_c n_c$; Acc_{high} : contracts with priority=3.

Method	Acc _{all} (%)	Acc _{high} (%)	PrioCovErr (%)
Indian+Salinas			
Rand	91.4 \pm 0.3	82.7 \pm 6.3	23.49 \pm 0.02
CB	90.0 \pm 1.3	87.9 \pm 4.7	31.35 \pm 0.05
OSAG-mix	91.2 \pm 0.5	88.3 \pm 6.4	11.76 \pm 0.05
EuroSAT			
Rand	84.1 \pm 0.2	80.8 \pm 4.9	24.08 \pm 0.07
CB	84.6 \pm 0.5	85.2 \pm 0.4	17.13 \pm 0.05
OSAG-mix	84.8 \pm 0.5	85.8 \pm 2.0	12.01 \pm 0.05

5.4 Baselines and OSAG policies

We compare:

- Rand: uniform random sampling (implicit frequency-based service).
- CB: class-balanced sampling (inverse-frequency) [9].
- OSAG: contract sampling with $\alpha = 1, \lambda_C = 0$.
- OSAG-mix: α -mix with $\alpha = 0.5$ and $\lambda_C = 0$.
- λ -fairloss: $\alpha = 1$ and $\lambda_C = 1$.

5.5 Metrics

We report Acc_{all} and Acc_{high} (in %), and $\text{PrioCovErr}(\%) = 100 \cdot \|\hat{q}_T - w\|_1$ (lower is better), averaged over three seeds.

6 Results and Analysis

6.1 Main trade-off results (Fig. 1 and Table 1)

Fig. 1 shows governance trade-off curves on Indian+Salinas and EuroSAT. The x -axis is priority coverage error (log scale, lower is better), and the y -axis is high-priority accuracy (higher is better). Markers show Rand, class-balanced (CB), OSAG, OSAG-mix, and λ -fairloss points. Table 1 summarizes the key operating points. OSAG improves governance (lower PrioCovErr) while maintaining global accuracy and improving high-priority accuracy.

Key observations: (i) Governance improves: PrioCovErr drops by $\approx 2\times$ on both datasets, consistent with Proposition 1. (ii) High-priority performance improves: Acc_{high} increases on both datasets. (iii) Global accuracy remains competitive: Acc_{all} changes only marginally under governance constraints.

6.2 Contract design matters: EuroSAT coarse vs. fine (Fig. 2)

The coarse-vs.-fine ablation supports Proposition 3: governance cost is influenced by contract structure. The fine design achieves comparable governance gain with a smaller empirical accuracy drop, consistent with Proposition 3’s contract-design effect.

7 Discussion, Limitations, and Practical Guidance

1. OSAG is governance, not a new backbone. Experiments intentionally use a simple MLP to show that governance gains are not tied to a specific architecture; OSAG can be combined with standard EO backbones (CNNs, transformers, spectral-spatial networks) that already achieve strong accuracy [8].
2. Contract design is part of the method. As highlighted by Proposition 3 and Fig. 2, contracts should align with operational semantics (region, mission strata, rare-but-important classes). Overly arbitrary partitions can increase within-contract heterogeneity or mismatch priorities and may increase the accuracy cost of governance.
3. Relation to imbalance and group robustness. Class-balanced methods [9] address label imbalance but do not enforce service targets over semantic groups. Group-robust methods optimize worst-case group risk [12] and fairness notions such as equal opportunity [17], while OSAG targets a policy-defined service distribution and monitors its compliance explicitly.
4. Limitations. The current study covers HSI and MSI, but not SAR or multimodal city-scale benchmarks. Extending OSAG to additional modalities and larger-scale geographic partitions is an important next step, as is integrating contract-graph construction from spatial adjacency or learned similarity.

8 Conclusion

We presented OSAG, a contract-governed training layer for EO that formalizes and controls who is served during training. With explicit targets over semantic contracts, OSAG reduces priority coverage error substantially, improves high-priority accuracy, and maintains competitive global accuracy on both HSI (Indian+Salinas) and MSI (EuroSAT). A EuroSAT coarse-vs.-fine ablation further shows that contract design modulates governance cost, consistent with a compact theoretical scaffold. OSAG offers a practical path toward policy-driven, accountable EO model training.

References

- [1] P. Helber, B. Bischke, A. Dengel, and D. Borth, “Introducing EuroSAT: A novel dataset and deep learning benchmark for land use and land cover classification,” *IGARSS 2018*, pp. 204–207, 2018, doi: 10.1109/IGARSS.2018.8519248.
- [2] M. Drusch, U. Del Bello, S. Carlier *et al.*, “Sentinel-2: ESA’s optical high-resolution mission for GMES operational services,” *Remote Sens. Environ.*, vol. 120, pp. 25–36, 2012.
- [3] R. O. Green, M. L. Eastwood, C. M. Sarture *et al.*, “Imaging spectroscopy and the Airborne Visible/Infrared Imaging Spectrometer (AVIRIS),” *Remote Sens. Environ.*, vol. 65, no. 3, pp. 227–248, 1998.
- [4] A. Plaza, J. A. Benediktsson, J. W. Boardman *et al.*, “Recent advances in techniques for hyperspectral image processing,” *Remote Sens. Environ.*, vol. 113, suppl. 1, pp. S110–S122, 2009.
- [5] P. Ghamisi, N. Yokoya, J. Li *et al.*, “Advances in hyperspectral image and signal processing: A comprehensive overview of the state of the art,” *IEEE Geosci. Remote Sens. Mag.*, vol. 5, no. 4, pp. 37–78, 2017.

- [6] Y. Li, H. Zhang, and Q. Shen, “Spectral–spatial classification of hyperspectral imagery with 3D convolutional neural network,” *Remote Sens.*, vol. 9, no. 1, art. 67, 2017.
- [7] Z. Zhong, J. Li, Z. Luo, and M. Chapman, “Spectral–spatial residual network for hyperspectral image classification: A 3-D deep learning framework,” *IEEE Trans. Geosci. Remote Sens.*, vol. 56, no. 2, pp. 847–858, 2018.
- [8] X. X. Zhu, D. Tuia, L. Mou *et al.*, “Deep learning in remote sensing: A comprehensive review and list of resources,” *IEEE Geosci. Remote Sens. Mag.*, vol. 5, no. 4, pp. 8–36, 2017.
- [9] Y. Cui, M. Jia, T.-Y. Lin, Y. Song, and S. Belongie, “Class-balanced loss based on effective number of samples,” *CVPR 2019*, pp. 9260–9269.
- [10] Y. Bengio, J. Louradour, R. Collobert, and J. Weston, “Curriculum learning,” *ICML 2009*, pp. 41–48.
- [11] T. Schaul, J. Quan, I. Antonoglou, and D. Silver, “Prioritized experience replay,” *ICLR 2016*.
- [12] S. Sagawa, P. W. Koh, T. B. Hashimoto, and P. Liang, “Distributionally robust neural networks for group shifts: On the importance of regularization for worst-case generalization,” *ICLR 2020*.
- [13] A. Agarwal, A. Beygelzimer, M. Dudik, J. Langford, and H. Wallach, “A reductions approach to fair classification,” *ICML 2018*, pp. 60–69.
- [14] A. Cotter, M. Gupta, H. Jiang *et al.*, “Training well-generalizing classifiers for fairness metrics and other constraints,” *ICML 2019*, pp. 1397–1405.
- [15] I. Loshchilov and F. Hutter, “Decoupled weight decay regularization,” *ICLR 2019*.
- [16] D. P. Kingma and J. Ba, “Adam: A method for stochastic optimization,” *ICLR 2015*.
- [17] M. Hardt, E. Price, and N. Srebro, “Equality of opportunity in supervised learning,” *NeurIPS 2016*, pp. 3323–3331.
- [18] R. Jain, D.-M. Chiu, and W. Hawe, *A quantitative measure of fairness and discrimination for resource allocation in shared computer systems*, DEC Research Report TR-301, 1984.

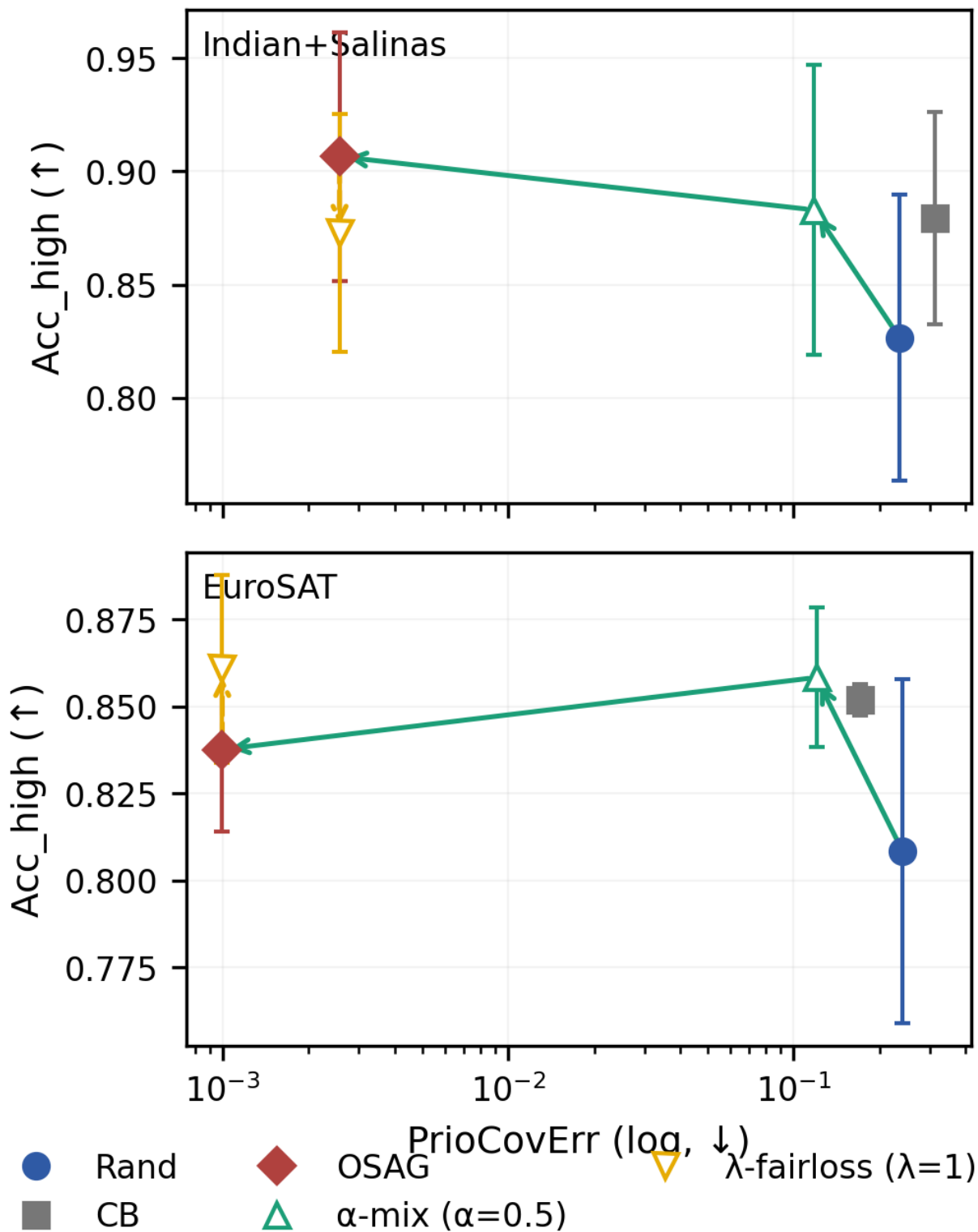


Figure 1: Governance trade-off on Indian+Salinas and EuroSAT: Acc_{high} vs. $PrioCovErr$ (log, lower is better). Error bars show std over 3 seeds.

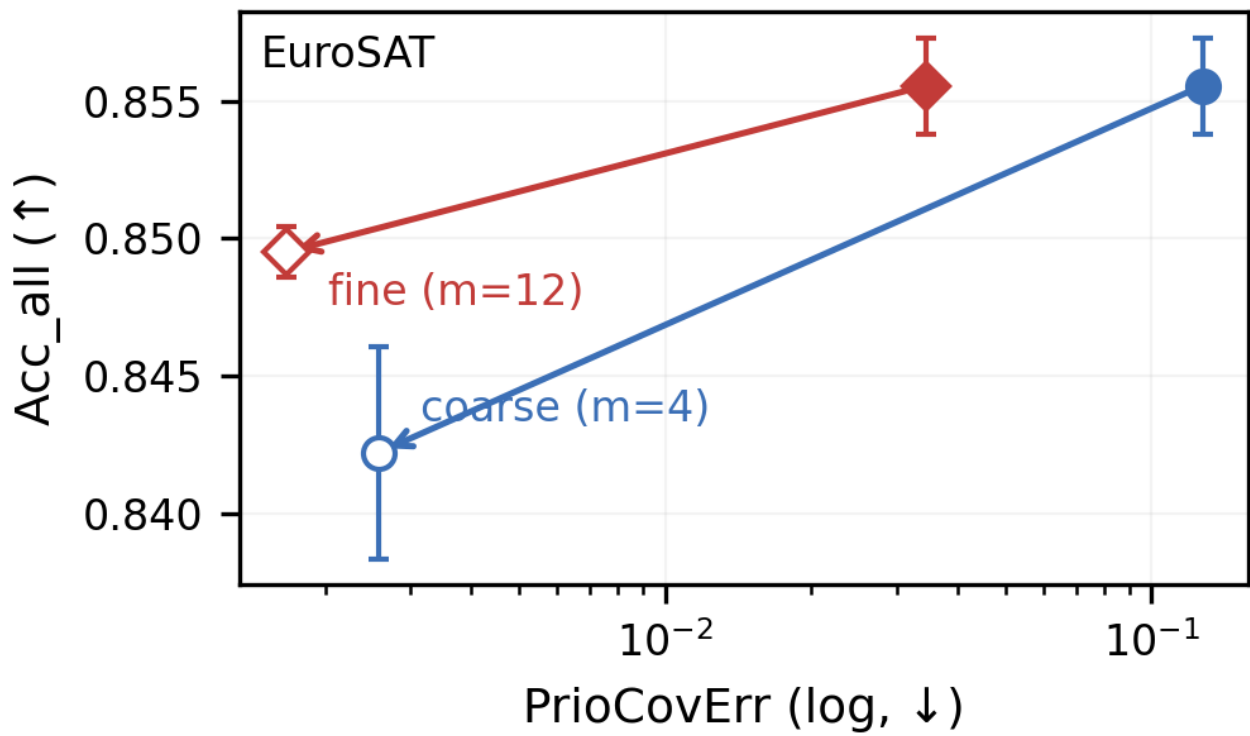


Figure 2: EuroSAT coarse vs. fine contracts: baseline \rightarrow OSAG arrows in (PrioCovErr, Acc_{all}).